Supporting Material

Hypertrophy-driven adipocyte death overwhelms recruitment under prolonged weight gain

Junghyo Jo, Juen Guo, Teresa Liu, Shawn Mullen, Kevin D. Hall, Samuel W. Cushman, and Vipul Periwal

Supplemental Methods

Experimental Procedures

Measurement of body composition

Body composition was measured once per week using 1H NMR spectroscopy (EchoMRI 3-in-1, Echo Medical Systems LTD, Houston, TX) after body weight was determined. At 0, 7, and 19 weeks, 6 mice from each group were randomly selected and euthanized by cervical dislocation after intraperitoneal administration of Ketamine/xylazine (0.1 mg Ketamine mixed with 0.01 mg xylazine per body weight 1 g) between 9 and 11 am. We measured epididymal, inguinal, retroperitoneal, and mesenteric fat pad mass to 0.1 mg precision.

Measurement of cell-size in fat pads

Adipose cell-size distributions in fat pads were measured using a Coulter counter (Multisizer III; Beckman Coulter, Miami, FL), as previously described (1). Briefly, two samples of 20 to 30 mg of tissue were immediately fixed in osmium tetroxide and incubated in a water bath at 37 °C for 48 h, and then adipose cell-size was determined by the Multisizer with a 400 μm aperture. The effective cell-size range using this aperture is 20 to 240 μm. To exclude possible contamination from particles that are not adipose cells, we considered sizes above 25 μm. The instrument was set to count 6,000 particles, and the fixed-cell suspension was diluted so that coincident counting was less than 10%. After collection of pulse sizes, the data were expressed as particle diameters and displayed as histograms of counts against diameter using linear bins and a linear scale for the x-axis. A sample was taken from each fat pad and processed separately. Each sample was then counted at least twice. The curves from the two samples were then averaged, but only after examining the reproducibility between the two samples.

Computational Methods

Tissue mass, mean cell size, and total cell number

For given absolute frequencies $n(s, t)$ of adipose cell size at time t, it is straightforward to calculate fat pad mass m, volume-weighted mean cell-

size $\bar{s}$, and total cell number n_{tot}:

$$m = \rho \int \frac{4\pi}{3} \left(\frac{s}{2}\right)^3 n(s,t)ds,$$

$$\bar{s} = \frac{\int ss^3 n(s,t)ds}{\int s^3 n(s,t)ds},$$

$$n_{tot} = \int n(s,t)ds.$$

Here $\rho = 0.915$ g/ml is adipose tissue density (2).

Numerical solution of partial differential equation

We solved the following discrete version of our model, given as continuous partial differential equations. The discrete weight gain model of Eq. (1) is

$$n(s_i, t_{j+1}) = n(s_i, t_j) + \delta t b \delta_{i,0} + \delta t[v(s_{i-1}, t_j)n(s_{i-1}, t_j) - v(s_i, t_j)n(s_i, t_j)]$$
$$+\delta t D[n(s_{i-1}, t_j) + n(s_{i+1}, t_j) - 2n(s_i, t_j)] - \delta t k(s_i) H(\bar{s} - \bar{s}_c)n(s_i, t_j)$$

with time interval δt=0.01 week and size interval $\delta s = s_i - s_{i-1}$ =0.73 μm. Here the Kronecker delta $\delta_{i,0}$ gives 1 only if i=1, otherwise 0. Next the discrete alternative weight loss model of Eq. (5) is

$$n(s_i, t_{j+1}) = n(s_i, t_j) + \delta t[v(s_{i+1}, t_j)n(s_{i+1}, t_j) - v(s_i, t_j)n(s_i, t_j)]$$
$$+\delta t D[n(s_{i-1}, t_j) + n(s_{i+1}, t_j) - 2n(s_i, t_j)] - \delta t k(s_i)n(s_i, t_j).$$

Then, the discrete original weight loss model of Eq. (4) is the same with this discrete form except for $k(s_i) = 0$.

Optimization method

From the initial and final absolute cell-size frequencies, $n(s, t_0)$ and $n(s, t_f)$, we deduced model parameters: $\vec{x}$=$(b,v_m,s_l,\eta_l,s_u,\eta_u,\Delta,D,k_m,s_k,\eta_k)$ for weight gain and $\vec{x}$=$(v_m,s_l,\eta_l,s_u,\eta_u,\Delta,D)$ for weight loss. For the alternate models of weight gain and loss including cell death, we used $\vec{x}$=$(b,v_m,s_l,\eta_l,s_u,\eta_u,\Delta,D,k_m)$ and $\vec{x}$=$(v_m,s_v,\eta_v,D,k_m,s_k,\eta_k)$, respectively. To optimize these model parameters, we used a minimization of "cost" quantifying a deviation between the measured final distribution $n(s_i, t_f)$ and a simulated final distribution $\hat{n}(s_i, t_f; \vec{x})$ with a given parameter set $\vec{x}$:

$$E = \sum_{i=1}^{l-1} \frac{[n(s_i, t_f) - \hat{n}(s_i, t_f; \vec{x}]^2}{\sigma^2},$$

where l is the total number of cell size bins. The scale σ^2 of the cost function was calculated from the intrinsic fluctuation of experimental data, which could be defined as the squared deviation between the measured final cell-size distribution $n(s_i, t_f)$ and its smoothed function $\tilde{n}(s_i, t_f)$:

$$\sigma^2 = \sum_{i=1}^{l-1} [n(s_i, t_f) - \tilde{n}(s_i, t_f)]^2.$$

Here we used the Double Exponential Smoothing method (Holt's method) (3):

$$\begin{aligned} \tilde{n}_i &= an_i + (1-a)(\tilde{n}_{i-1} + y_{i-1}) \\ y_i &= b(\tilde{n}_i - \tilde{n}_{i-1}) + (1-b)y_{i-1}, \end{aligned}$$

where for simplicity, we abbreviated $n(s_i, t_f)$ and $\tilde{n}(s_i, t_f)$ as n_i and $\tilde{n}_i$, respectively; initial values are $\tilde{n}_0 = n_0$ and $y_0 = n_1 - n_0$; two constants are $a = b = 0.3$.

For the parameter optimization, we used the parallel tempering Monte-Carlo (MC) method to find the global minimum of the cost function (4). We set 10 uniformly spaced values (0.1 to 1) for the tempering parameter Θ_i and ran 10 chains (i=1,2,...,10) in parallel with updating probability $\exp[-\Theta_i E(\vec{x}_i)]$. At every 20 steps, we randomly picked two chains of different temperatures (Θ_i and Θ_j) and exchanged their parameter sets ($\vec{x}_i$ and $\vec{x}_j$) with probability $\exp[(\Theta_i - \Theta_j)(E_i - E_j)]$, where E_i and E_j are $E(\vec{x}_i)$ and $E(\vec{x}_j)$, to find the global minimum of the cost more efficiently. After equilibration, we calculated likelihood values of parameters and cost by averaging the parameters and cost generated by 10^5 MC steps with a fixed temperature $\Theta = 1$. For the model comparison, we used the Bayesian model probability $P(M|D)$, which estimates how well a model describes given data (4). The probability can be calculated from the MC simulation with different temperatures: for 10 chains, $-\ln P(M|D) = 1/10 \sum_{i=1}^{10} \bar{E}_i$, where $\bar{E}_i$ represents the average cost for each temperature Θ_i. Note that for this calculation, there is no exchange between MC chains of different temperatures in contrast to the previous procedure for searching a global minimum of a cost function. In addition, we used 10^5 MC steps to determine the model probability .

References

1. McLaughlin, T., A. Sherman, P. Tsao, O. Gonzalez, G. Yee, C. Lamedola, G. M. Reaven, and S. W. Cushman, 2007. Enhanced proportion of small

adipose cells in insulin-resistant vs insulin-sensitive obese individuals implicates impaired adipogenesis. *Diabetologia* 50:1707–1715.

2. Lemonnier, D., 1972. Effect of age, sex, and site on the cellularity of the adipose tissue in mice and rats rendered obese by a high-fat diet. *J. Clin. Inv.* 51:2907–2915.

3. Gardner, E. S., 2006. Exponential smoothing: The state of the art–Part II. *International Journal of Forecasting* 22:637–666.

4. Gregory, P. C., 2005. Bayesian logical data analysis for the physical sciences: a comparative approach with mathematica support. Cambridge University Press, Cambridge, UK, first edition.

Supplemental Tables

Table S1A. Model parameters for epididymal fat.

	7wN	7wHF	7wE	19wN	19wHF	19wE	7wHF +12wN	7wE +12wN
b [$\times 10^5$/week]	6.6±4.1	13.1±2.4	8.5±4.4	0.4±0.3	6.3±3.1	4.8±2.8	-	-
v_m [μm/week]	2.4±0.9	2.0±0.2	2.2±0.6	1.6±0.7	2.2±0.1	2.0±0.1	-5.0±1.8*	-4.3±1.4*
s_l [μm]	26±6	34±1	35±5	35±5	32±2	30±2	22.9±0.4	23±1
η_l [μm]	10±8	19±1	19±2	16±1	18±1	17±1	6±1	6±1
s_u [μm]	68±18	94±3	93±3	82±5	97±7	93±6	58±8	68±10
η_u [μm]	28±21	50±2	51±2	41±15	53±4	53±4	33±16	32±19
Δ	4.2±1.1	5.9±0.7	6.2±1.5	3.1±1.2	6.2±0.7	5.8±1.1	1.7±0.7	2.4±1.0
k_m [week^{-1}]	-	-	-	-	1.4±0.2	1.3±0.2	-	-
s_k [μm]	-	-	-	-	183±6	176±15	-	-
η_k [μm]	-	-	-	-	325±29	282±55	-	-
$\bar{s}_c$ [μm]	-	-	-	-	126±3	120±6	-	-
D [μm^2/week]	11±7	16±1	15±2	11±3	14±1	15±1	5±3	8±5
E (cost)	8.3±6.5	3.0±0.6	2.9±0.7	5.3±1.1	3.6±0.6	3.2±0.8	5.4±1.5	4.7±1.2

Summarized are model parameters depending on diet: recruitment rate b, growth/shrinkage rate $v(s) = v_m/4[1 + \tanh((s - s_l)/\eta_l)][\Delta - \tanh((s - s_u)/\eta_u)]$, death rate $k(s)H(\bar{s} - \bar{s}_c)$ with $k(s) = k_m/2[1 + \tanh((s - s_k)/\eta_k)]$, and fluctuation rate D. Abbreviations of diet are 7-week normal diet (7wN), 7-week high-fat diet (7wHF), 7-week Ensure diet (7wE), 19-week normal diet (19wN), 19-week high-fat diet (19wHF), 19-week Ensure diet (19wE), 7-week high-fat diet plus 12-week normal diet (7wHF+12wN), and 7-week Ensure diet plus 12-week normal diet (7wE+12wN). Note that cell death parameters are only in long-term high-fat diet (19wHF and 19wE), and recruitment parameters are not necessary under the weight loss (7wHF+12wN and 7wE+12wN). Mean ± SD of parameter values are calculated from six likelihood parameter values (N=6); the likelihood parameter value for a given sample is obtained from 10^5 Monte-Carlo steps starting from the most likelihood parameter set giving the minimal cost. *The minus sign represents cell shrinkage, opposite to growth.

Table S1B. Model parameters for inguinal fat.

	7wN	7wHF	7wE	19wN	19wHF	19wE	7wHF +12wN	7wE +12wN
b $[\times 10^5/\text{week}]$	4.5±3.0	17.5±8.3	9.7±5.3	0.6±0.2	9.3±4.9	3.8±1.9	-	-
v_m $[\mu\text{m/week}]$	2.3±0.5	2.2±0.4	1.9±0.5	0.8±0.5	1.9±0.4	1.7±0.2	-5.1±7.4	-2.2±2.4
s_l $[\mu\text{m}]$	23±1	25±2	30±6	30±5	31±4	32±3	29±10	28±9
η_l $[\mu\text{m}]$	8±2	13±3	16±3	16±1	18±1	17±2	5±1	5±1
s_u $[\mu\text{m}]$	62±9	77±18	88±8	68±13	88±5	94±8	65±26	67±24
η_u $[\mu\text{m}]$	28±12	41±17	46±2	38±11	50±4	51±1	36±24	42±22
Δ	3.2±0.7	4.9±1.5	5.5±0.7	2.9±0.7	5.8±0.8	4.9±0.7	3.0±1.4	3.5±1.1
k_m $[\text{week}^{-1}]$	-	-	-	-	1.4±0.3	1.4±0.3	-	-
s_k $[\mu\text{m}]$	-	-	-	-	178±16	192±22	-	-
η_k $[\mu\text{m}]$	-	-	-	-	271±79	261±63	-	-
$\bar{s}_c$ $[\mu\text{m}]$	-	-	-	-	106±4	105±1	-	-
D $[\mu\text{m}^2/\text{week}]$	9±4	12±3	15±1	9±7	14±1	15.9±0.3	13±4	11±2
E (cost)	5.4±1.3	5.5±1.0	5.5±2.5	4.1±0.9	3.6±0.5	3.9±0.7	3.7±0.8	4.3±1.3

Table S1C. Model parameters for retroperitoneal fat.

	7wN	7wHF	7wE	19wN	19wHF	19wE	7wHF +12wN	7wE +12wN
$b\ [\times 10^5/\text{week}]$	0.3±0.2	6.3±3.0	4.8±2.3	0.4±0.4	2.9±2.1	4.1±2.6	-	-
$v_m\ [\mu\text{m/week}]$	1.4±0.4	2.1±0.4	2.3±0.4	1.1±0.7	1.6±0.9	1.2±0.8	-3.6±2.5	-4.6±1.4
$s_l\ [\mu\text{m}]$	33±8	32±2	31±4	33±5	31±5	33±4	23±1	22.6±0.5
$\eta_l\ [\mu\text{m}]$	16±3	19±1	19±2	17±2	16±3	18±1	5±1	5±1
$s_u\ [\mu\text{m}]$	83±13	94±3	96±3	73±19	86±11	89±6	60±19	73±19
$\eta_u\ [\mu\text{m}]$	48±8	48±1	49±1	41±18	48±6	52±6	36±18	35±20
Δ	4.4±1.1	6.1±0.6	6.2±1.0	3.6±1.6	5.0±1.9	5.3±1.2	2.9±1.3	2.4±0.6
$k_m\ [\text{week}^{-1}]$	-	-	-	-	1.6±0.2	1.7±0.5	-	-
$s_k\ [\mu\text{m}]$	-	-	-	-	183±21	168±19	-	-
$\eta_k\ [\mu\text{m}]$	-	-	-	-	251±70	287±14	-	-
$\bar{s}_c\ [\mu\text{m}]$	-	-	-	-	123±7	122±3	-	-
$D\ [\mu\text{m}^2/\text{week}]$	15±3	15±1	14±2	15±3	13±1	14.6±0.5	9±2	11±3
E (cost)	4.8±1.4	3.1±0.8	3.0±0.7	4.8±1.4	3.5±0.8	3.2±1.1	5.4±1.6	5.3±1.1

Table S1D. Model parameters for mesenteric fat.

	7wN	7wHF	7wE	19wN	19wHF	19wE	7wHF +12wN	7wE +12wN
$b\ [\times 10^5/\text{week}]$	2.8±4.6	5.1±2.8	6.2±3.8	0.5±0.5	12.2±21.9	10.5±17.3	-	-
$v_m\ [\mu\text{m/week}]$	2.0±0.6	1.9±0.7	2.1±0.5	1.9±1.4	2.3±0.2	1.7±0.7	-9.6±4.9	-9.4±3.2
$s_l\ [\mu\text{m}]$	31±9	31±7	33±8	29±5	29±3	32±5	23±1	24±1
$\eta_l\ [\mu\text{m}]$	13±3	16±6	19±3	13±5	18±2	18±3	6±1	6.2±0.4
$s_u\ [\mu\text{m}]$	73±23	81±18	93±2	65±11	95±12	89±4	42±7	47±7
$\eta_u\ [\mu\text{m}]$	37±22	40±18	51±2	28±22	49±4	54±5	20±15	15±6
Δ	3.7±1.4	4.6±0.8	6.2±1.1	2.2±1.2	6.8±0.3	6.1±0.4	1.4±0.3	1.7±0.5
$k_m\ [\text{week}^{-1}]$	-	-	-	-	1.7±0.3	1.8±0.3	-	-
$s_k\ [\mu\text{m}]$	-	-	-	-	198±24	181±8	-	-
$\eta_k\ [\mu\text{m}]$	-	-	-	-	232±80	279±54	-	-
$\bar{s}_c\ [\mu\text{m}]$	-	-	-	-	112±11	111±13	-	-
$D\ [\mu\text{m}^2/\text{week}]$	9±7	12±5	15±2	7±6	14±1	14±1	12±3	4±3
E (cost)	6.5±7.7	4.7±2.0	4.0±2.1	7.2±8.0	4.0±1.2	3.7±1.0	4.8±1.1	4.4±0.8

Table S2. Model parameters for an alternative model of prolonged weight gain.

	epididimal		inguinal		retroperitoneal		mesenteric	
	19wHF	19wE	19wHF	19wE	19wHF	19wE	19wHF	19wE
$b \ [\times 10^5/\text{week}]$	6.0±3.8	4.4±3.1	10.2±7.3	2.9±1.0	2.0±1.5	4.0±3.1	14.7±29.7	14.3±26.2
$v_m \ [\mu\text{m/week}]$	1.6±0.3	1.5±0.3	2.0±0.2	1.4±0.3	1.6±0.8	1.1±0.5	2.0±0.5	1.5±0.6
$s_l \ [\mu\text{m}]$	35±3	33±4	32±4	34±2	32±5	33±3	33±5	33±6
$\eta_l \ [\mu\text{m}]$	19±3	18±2	18±3	18±2	16±2	17±3	18±4	20±3
$s_u \ [\mu\text{m}]$	92±9	95±13	90±12	86±4	86±13	88±4	101±8	97±12
$\eta_u \ [\mu\text{m}]$	53±5	52±5	47±5	51±5	43±9	43±6	52±11	54±9
Δ	5.7±0.7	5.4±1.0	4.6±1.0	4.6±0.9	3.1±1.7	4.2±1.1	5.6±0.6	5.3±1.5
$k_m \ [\text{week}^{-1}]$	0.7±0.3	0.5±0.3	0.8±0.3	0.4±0.2	1.5±1.0	1.6±0.8	0.5±0.2	0.9±0.3
$\bar{s}_c \ [\mu\text{m}]$	126±3	119±6	110±5	105±2	124±7	125±4	108±13	113±11
$D \ [\mu\text{m}^2/\text{week}]$	16±1	16±2	14±2	17±1	13±4	15±1	16±1	16±3
E (cost)	3.4±0.4	3.6±1.1	3.8±0.5	4.1±0.7	3.5±0.6	3.3±1.1	4.6±1.6	4.1±1.2
$\ln[P(M_1\|D)$	0.60	1.23	0.92	0.99	0.11	-0.19	1.00	0.79
$/P(M_2\|D)]$	±0.42	±0.80	±0.27	±0.54	±0.69	±0.24	±0.56	±0.57
P value	0.018	0.026	<0.001	0.015	0.708	0.156	0.007	0.036

The alternative model (Model 2) assumes size-independent cell death under prolonged high-fat and Ensure diet, while the original model (Model 1) assumes size-dependent cell death. Bayesian model comparison is performed, and each model probability for a given data is calculated as log values of relative model probabilities (see the Supporting Material for the detail of the calculation). Here P value represents paired Student's t-test between two model probabilities.

Table S3. Model parameters for an alternative model of diet switch from high-fat to normal.

	epididimal		inguinal		retroperitoneal		mesenteric	
	7wHF +12wN	7wE +12wN	7wHF +12wN	7wE +12wN	7wHF +12wN	7wE +12wN	7wHF +12wN	7wE +12wN
v_m [μm/week]	1.1±0.5	1.4±0.7	0.7±0.5	0.8±0.4	1.6±0.8	2.2±0.8	1.0±0.6	2.1±0.6
s_v [μm]	29±4	28±3	33±3	33±5	30±6	31±9	30±4	28±2
η_v [μm]	6±1	6±1	6±1	5.8±0.5	5±1	6±1	6±1	5±1
k_m [week^{-1}]	0.3±0.2	0.3±0.1	0.7±0.5	0.3±0.3	0.8±0.9	0.2±0.1	0.8±0.9	1.0±1.1
s_k [μm]	59±23	72±29	88±48	112±21	60±40	103±41	64±34	33±13
η_k [μm]	57±59	152±98	188±125	284±40	98±107	265±112	128±105	34±17
D [μm^2/week]	7±3	8±7	13±4	12±5	10±4	13±5	11±6	5±4
E (cost)	6.4±1.8	5.6±1.4	3.7±1.4	4.7±1.7	5.4±1.1	5.6±1.0	5.7±1.2	5.4±1.1
$\ln[P(M_1|D)$ /$P(M_2|D)]$	3.25 ±0.34	2.61 ±1.14	0.59 ±1.99	0.63 ±1.50	1.85 ±1.22	0.69 ±0.63	1.51 ±1.47	3.30 ±1.09
P value	< 0.001	0.002	0.503	0.349	0.014	0.043	0.053	0.001

The alternative model (Model 2) assumes simpler size-dependent cell growth, $v(s) = v_m/2[1+\tanh((s-s_v)/\eta_v)]$, and includes cell death, $k(s) = k_m/2[1-\tanh((s-s_k)/\eta_k)]$, differently form the original model (Model 1). Bayesian model comparison is performed, and each model probability $P(M_{1,2}|D)$ for a given data is calculated as log values of relative model probabilities. Here P value represents paired Students t-test between two model probabilities.
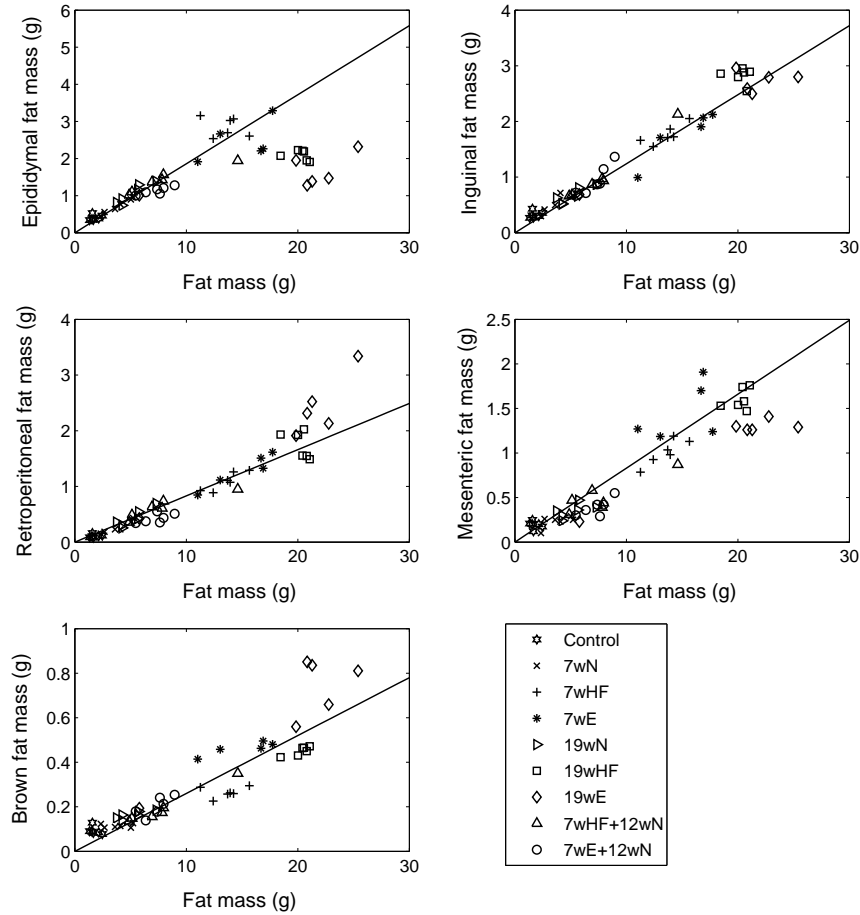
Supplemental Figures

Fig. S1. Linear relationship between body fat mass and fat pad mass. Epididymal, inguinal, retroperitoneal, mesenteric, and brown fat mass is linear except for long-term high-fat and the Ensure diet. Each symbol represents individual mice: 3 months old, male, C57BL/6 mice (Control), after 7-week normal diet (7wN), 7-week high-fat diet (7wHF), 7-week Ensure diet (7wE), 19-week normal diet (19wN), 19-week high-fat diet (19wHF), 19-week Ensure diet (19wE), 7-week high-fat plus 12-week normal diet (7wHF+12wN), and 7-week Ensure diet plus 12-week normal diet. For the linear regression, data of Control, 7wN, 7wHF, and 7wE are used because the linear relation between fat pad mass and body fat mass was used to estimate fat pad mass at week 7.
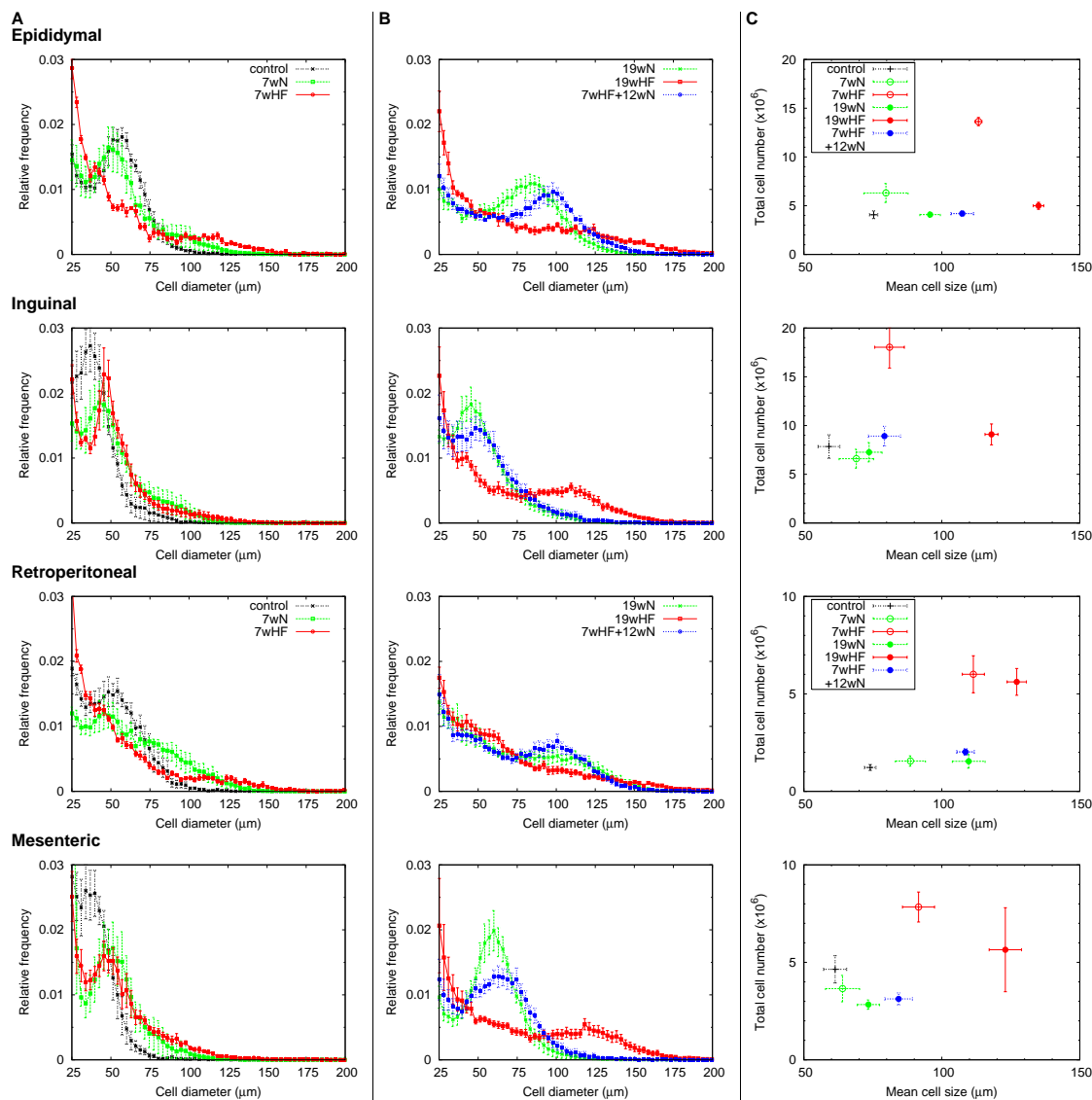
Fig. S2. Adipose cell-size distributions in epididymal, inguinal, retroperitoneal, and mesenteric fat under different diet. (A) Relative frequencies of adipose cell diameters at initial time (control), after 7-week normal diet (7wN), and after 7-week high-fat diet (7wHF) are plotted. (B) The ones after 19-week normal diet (19wN), after 19-week high-fat diet (19wHF), and after 7-week high-fat plus 12-week normal diet (7wHF+12wN). (C) Based on these relative frequencies of cell size and fat pad mass, volume-weighted mean cell size (hypertrophy index) and total cell number (hyperplasia index) are estimated. N=6. Their absolute values are summarized in Table 1. Note that the total cell number is counted from adipose cells of which diameter is larger than 25 μm.
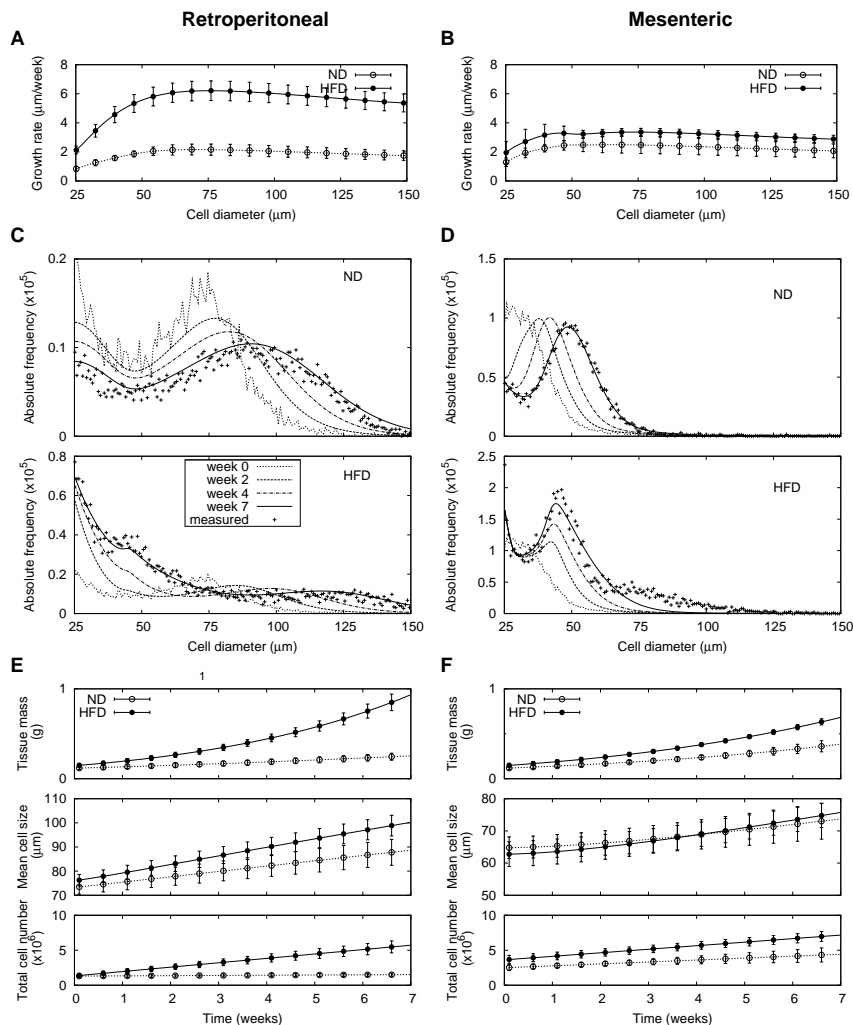
Fig. S3. Adipose tissue growth under 7-week normal and high-fat diets. Size-dependent growth rates of adipose cells are deduced from changes of cell-size distributions in (A) retroperitoneal and (B) mesenteric fat under normal (ND) and high-fat diets (HFD). The plotted growth rates are mean results estimated from likelihood values of six mice (Tables S1C and S1D). Changes of adipose cell-size distribution for (C) retroperitoneal and (D) mesenteric fat under normal and high-fat diets in a representative mouse among six mice are predicted by the mathematical model. Here the most likelihood initial cell-size distributions and model parameters are used (see Methods and Supporting Material for detail). Note that absolute frequencies of adipose cell size are estimated by using measured relative frequencies of adipose cell size and mass of dissected fat depots. Measured final cell-size distributions are expressed with the plus symbol (+). Based on the model predictions of cell-size distribution, time trajectories of tissue mass, volume-weighted mean cell size, and total cell number are estimated for (E) retroperitoneal and (F) mesenteric fat (N=6).
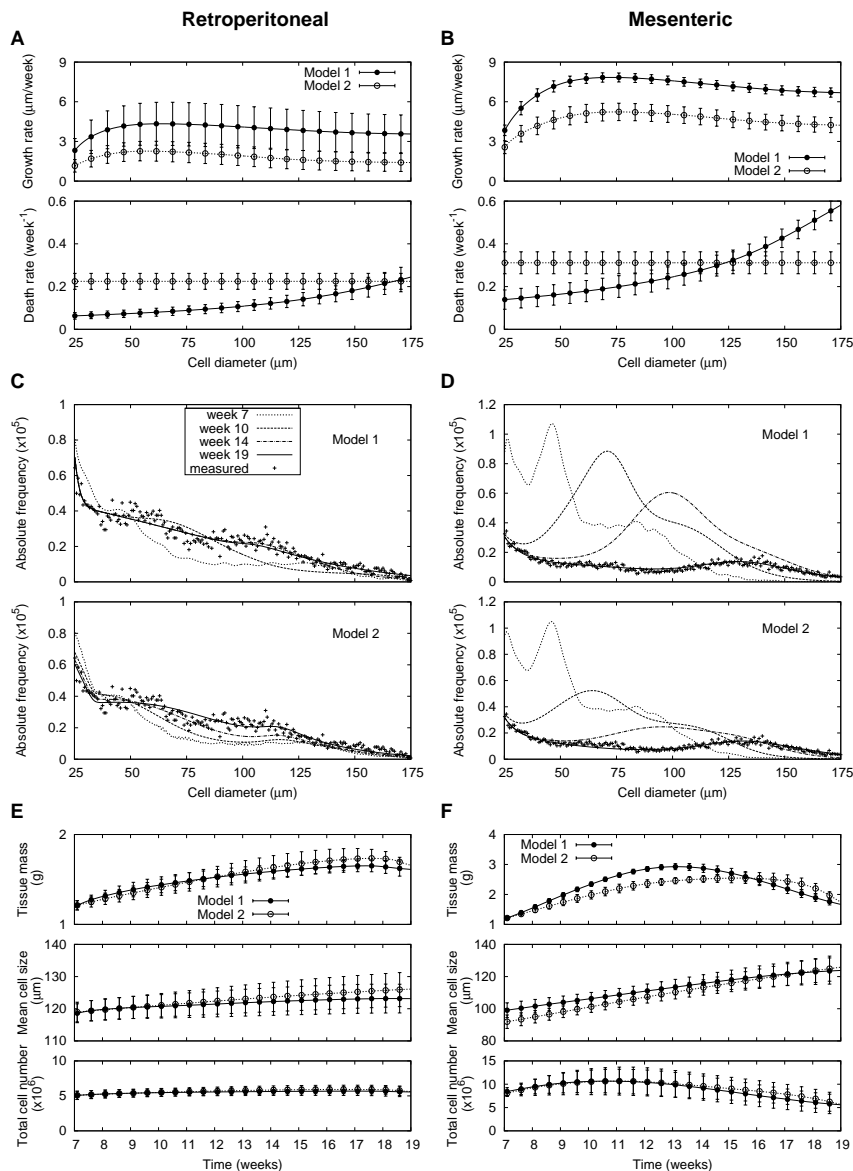
Fig. S4. Adipose tissue growth under 19-week high-fat diet. Size-dependent growth and death rates in two models are deduced from changes of cell-size distributions in (A) retroperitoneal and (B) mesenteric fat (N=6; Tables S1C and S1D). Changes of adipose cell-size distribution for (C) retroperitoneal and (D) mesenteric fat under prolonged high-fat diet in a representative mouse among six mice are predicted by two mathematical models. For the initial cell-size distributions at week 7 after high-fat diet and model parametes, the most likelihood values are used. Measured final cell-size distributions are expressed with the plus symbol (+). Based on the model predictions of cell-size distribution, time trajectories of tissue mass, volume-weighted mean cell size, and total cell number are estimated for (E) retroperitoneal and (F) mesenteric fat (N=6).
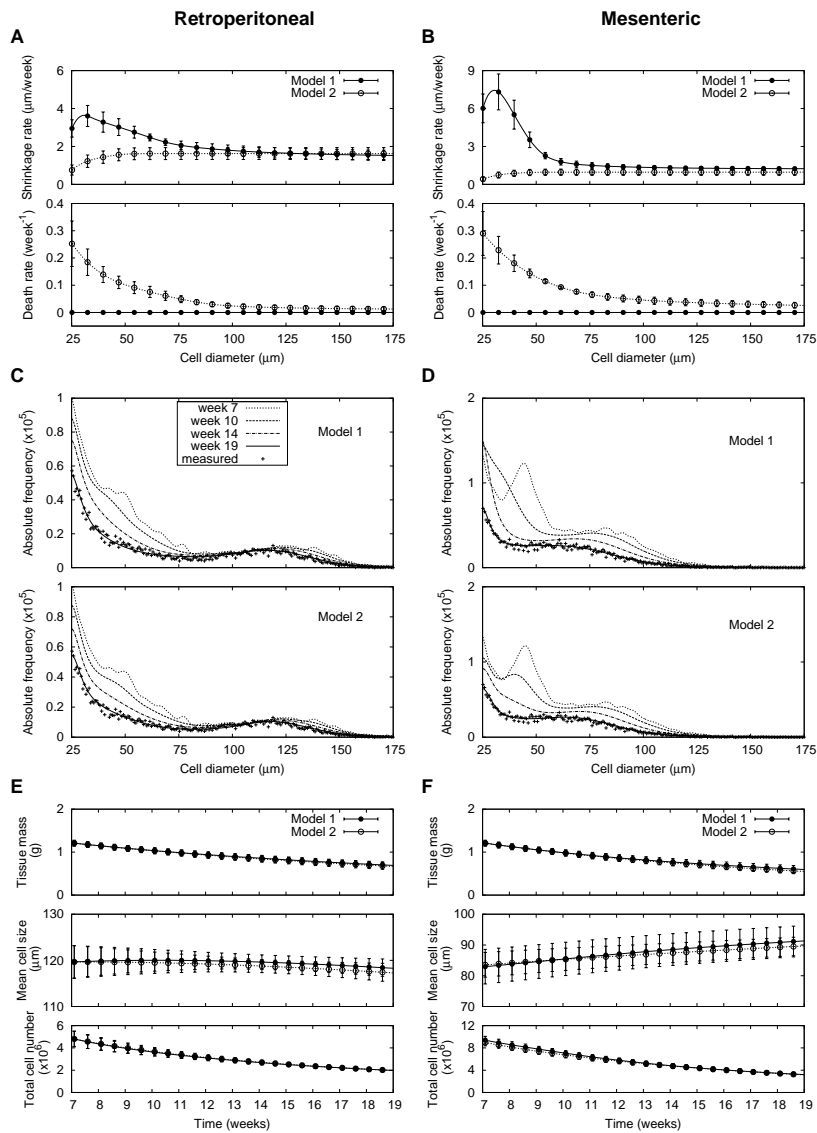
Fig. S5. Adipose tissue shrinkage under switch to 12-week normal diet after 7-week high-fat diet. Size-dependent shrinkage and death rates in two models are deduced from changes of cell-size distributions in (A) retroperitoneal and (B) Mesenteric fat (N=6; Tables S1C and S1D). Note that cell death is absent in the Model 1. Changes of adipose cell-size distribution for (C) retroperitoneal and (D) mesenteric fat under the diet switch in a representative mouse among six mice are predicted by two mathematical models. For the initial cell-size distributions at week 7 after high-fat diet and model parametes, the most likelihood values are used. Measured final cell-size distributions are expressed with the plus symbol (+). Here shrunken cells below the minimal diameter 25 μm are removed. Based on the model predictions of cell-size distribution, time trajectories of tissue mass, volume-weighted mean cell size, and total cell number are estimated for (E) retroperitoneal and (F) mesenteric fat (N=6).